

Supporting Information

Graphene-MnO₂ framework as a new generation of three-dimensional oxygen evolution promotor

Sheng Chen,^a Jingjing Duan,^a Wei Han^b and Shi Zhang Qiao^{*a}

^a School of Chemical Engineering, University of Adelaide, Adelaide, SA 5005, Australia. E-mail: s.qiao@adelaide.edu.au

^b Centre for Nano Scale Science and Technology, and School of Computer Science, Engineering, and Mathematics, Flinders University, Adelaide, SA 5042, Australia.

I. Experimental section

1. Chemicals

Graphite flakes, sulfuric acid (H₂SO₄, 95-98%), potassium permanganate (KMnO₄, 99%), phosphorus pentoxide (P₂O₅, 98%), potassium persulfate (K₂S₂O₈, 99%), potassium hydroxide (KOH, 99%), hydrogen peroxide (H₂O₂, 35 wt%), ethanol (EtOH, absolute), hydrochloric acid (HCl, 38 wt%), nickel nitrate (Ni(NO₃)₂·6H₂O, reagent grade), Iridium(IV) oxide (IrO₂, 99%), cobalt nitrate (Co(NO₃)₂·6H₂O, reagent grade) and urea (CH₄N₂O, reagent grade) were purchased from Sigma-Aldrich and directly used without further treatment or purification.

2. Preparation

Graphene oxide (GO) was prepared by chemical oxidation of natural graphite *via* Hummers' method,¹ which then formed a homogeneous dispersion by ultrasonication for ~30 min. The GO dispersion (2 mL, 2 mg mL⁻¹) was loaded into a Teflon-lined stainless steel autoclave and heated at 150 °C for 12 h to generate the 3D graphene framework (denoted as G). In the next step, G was oxidized with KMnO₄ to introduce MnO₂ nanoparticles on the sheets. Typically, G was merged with a solution of KMnO₄ (500 mg in 25 mL DI-water) at room temperature for 3 h. The as-resultant material, *i.e.*, graphene-MnO₂ framework (denoted as G-Mn), was collected and dialyzed against de-ionized (DI) water for 24 h.

Subsequently, G-Mn was used as the 3D scaffold for the controlled growth of NiCo₂O₄ to generate the hybrid catalyst. Specifically, 182 mg of Ni(NO₃)₂·6H₂O, 474 mg of Co(NO₃)₂·6H₂O and 720 mg of urea were dissolved into a mixed solution of ethanol (20 mL) and H₂O (20 mL). Then G-Mn was immersed into the above solution, and heated at 90 °C. The 3D hybrid material, *i.e.* graphene/MnO₂/NiCo₂O₄ (denoted as G-Mn-NiCo), was taken out after reaction for 3 h and annealed at 250 °C in furnace for 2 h.

For comparison, graphene-NiCo₂O₄ framework (denoted as G-NiCo) was prepared *via* a similar procedure to the preparation of G-Mn-NiCo in the absence of KMnO₄; NiCo₂O₄ was deposited into nickel foam (denoted as NiCo) by replacing G-Mn with a nickel foam.

3. Characterization

Powder X-ray diffraction (XRD) patterns were recorded on a Philips 1130 X-ray diffractometer (40 kV, 25 mA, Cu K α radiation, $\lambda=1.5418$ Å); Fourier transform infrared (FTIR) spectroscopy was recorded on a Nicolet 6700 spectrometer; ultraviolet-visible (UV-vis) spectroscopy was conducted on a SHIMADZU UV-2600 spectrophotometer; X-ray photoelectron spectroscopy (XPS) was obtained on an Axis Ultra (Kratos Analytical, UK) XPS spectrometer equipped with an Al K α source (1486.6 eV); morphologies of the samples were observed on transmission electron microscopy (TEM, Tecnai G2 Spirit) and scanning electron microscopy (SEM, QUANTA 450). The as-produced oxygen was analyzed using a gas chromatograph (GC-14C, Shimadzu, Japan, TCD, nitrogen as a carrier gas and 5 Å molecular sieve column).

MB adsorption experiments were used to probe the accessible surface areas of the samples. Specifically, the samples were put into a MB solution in ethanol (0.1 mg ml⁻¹) and were left at 25 °C for 24 h to allow the accessible surface of the samples to be maximally covered by MB molecules. The amount of the adsorbed MB was calculated from the concentration change of MB in the solution tested by UV-Vis spectra. The surface area was estimated according to the fact that each milligram of adsorbed MB occupies 2.45 m² of the surface area.^{2,3}

Pore size distribution, BET surface area and pore volume were evaluated by using nitrogen adsorption-desorption isotherms measured at 77 K on a TriStar II 3020 Micrometrics apparatus. The BET specific surface area was calculated using adsorption data at a relative pressure range of P/P₀ = 0.05-0.3. Pore size distribution was derived from the adsorption branch using the BJH method.^{4,5} The total pore volume was estimated from the adsorbed amount at a relative pressure (P/P₀) of 0.99.

4. Electrode preparation and electrochemical testing

Electrochemical measurements were performed in a standard three-electrode glass cell on a 760 workstation (Pine Research Instruments, US) using a Pt wire as a counter electrode and Ag/AgCl/KCl (3 M) as a reference electrode. Similar to the previous report,⁶ the working electrode was fabricated by

directly depositing catalysts into nickel foam without additional binders. Taking G-Mn-NiCo for an example, a piece of nickel foam sheet was firstly cleaned by ultrasonication in acetone, ethanol and DI-water, respectively. The nickel foam was then immersed into the GO dispersion (2 mL, 2 mg mL⁻¹), followed by sonication for 30 min to ensure the successful filling of the mixed solution into the micropores of nickel foam. Then the mixture was hydrothermally treated at 150 °C for 12 h to generate graphene framework in nickel foam. Next, the similar methods were performed for the oxidation of graphene with KMnO₄ and the controlled assembly of NiCo₂O₄ in G-Mn framework. For comparison purpose, IrO₂ was deposited into nickel foam by a drop-casting method. Specifically, IrO₂ (2 mg) was ultrasonically dispersed in Milli-Q water (1 mL) with Nafion (30 μL of 0.1%). Then, the catalyst dispersion was transferred onto the nickel foam and dried. Further, the catalytic performance of G-Mn-NiCo was tested on a 2D planar electrode (glass carbon electrode, denoted as 2D NG-NiCo). G-Mn-NiCo were firstly crushed into fine powder by using a mortar, and then prepared into catalyst dispersion (2 mg mL⁻¹) *via* a procedure similar to that of IrO₂. Next, the catalyst dispersion (7.2 μL) was transferred onto the glassy carbon electrode and dried, yielding a loading of 0.2 mg cm⁻² catalyst.

Linear scan voltammograms (LSV) and cyclic voltammetry (CV) were conducted with the scan rate of 5 mV s⁻¹; Tafel plots were obtained from 0.3 to 1 V; the chronoamperometric response of samples was obtained at 0.6 V *vs.* Ag/AgCl. The current density was normalized to the geometrical area and the measured potentials *vs.* Ag/AgCl can be converted to a reversible hydrogen electrode (RHE) scale according to the Nernst equation ($E_{\text{RHE}} = E_{\text{Ag/AgCl}} + 0.059 \text{ pH} + 0.197$). Faradaic efficiency of the reaction is estimated according to $\eta = zn/Q$, where η is Faradaic efficiency, z is electro-chemical equivalent, n is molarity of oxygen obtained from gas chromatography, and Q is the coulombic charge obtained from chronometric testing). The electrochemically active surface area (ESA) was measured according to the method reported in literature.^{7,8} Specifically, the electrode was cycled between 0 and 1 V (*vs.* Ag/AgCl) in a nitrogen saturated 0.1 M KOH solution at a rate of 50 mV/s. The ESA is estimated according to $\text{ESA} = Q/(540 \cdot m)$, where Q is the coulombic charge obtained from integrating the CV plots, 540 μC cm⁻² is the charge density associated with the formation of monolayer M(OH)₂ (M = Ni, Co), m is the catalyst loading.

II. Supplementary Results

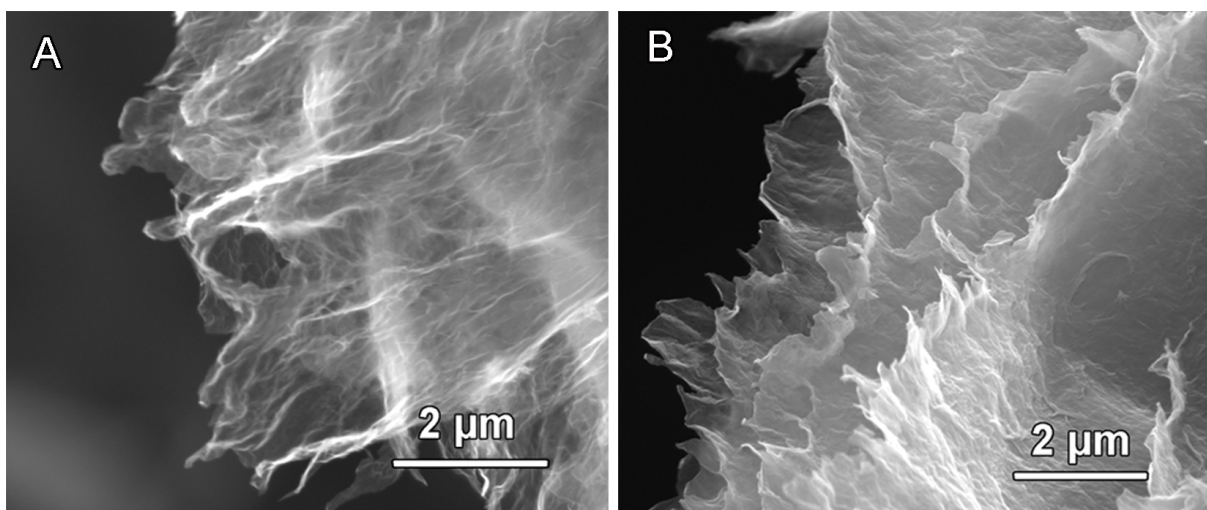


Figure S1. SEM images of graphene (A) and G-Mn (B).

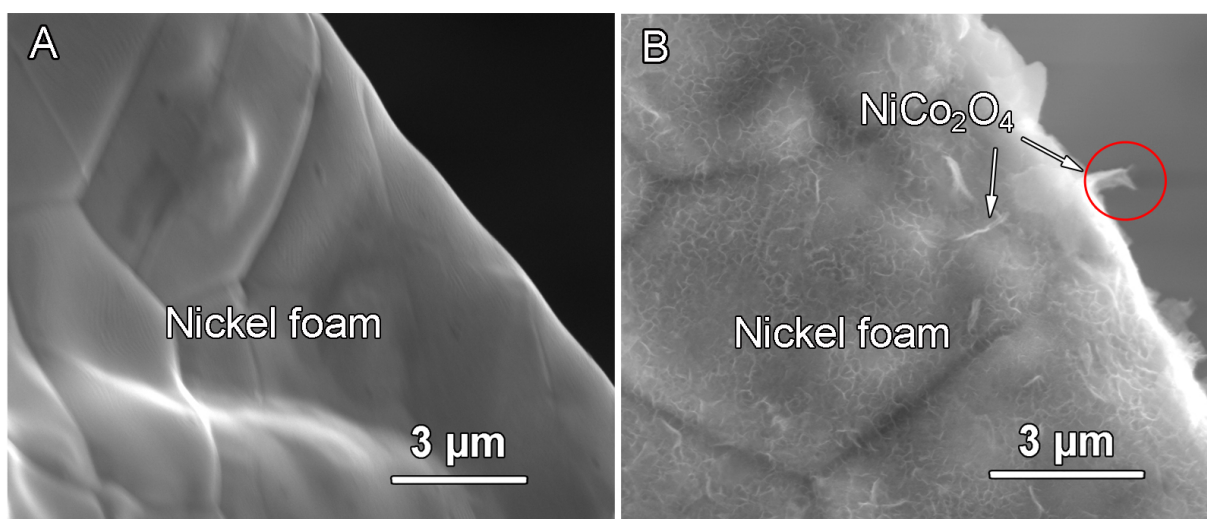


Figure S2. SEM images of nickel foam (A) and NiCo₂O₄ on nickel foam (B).

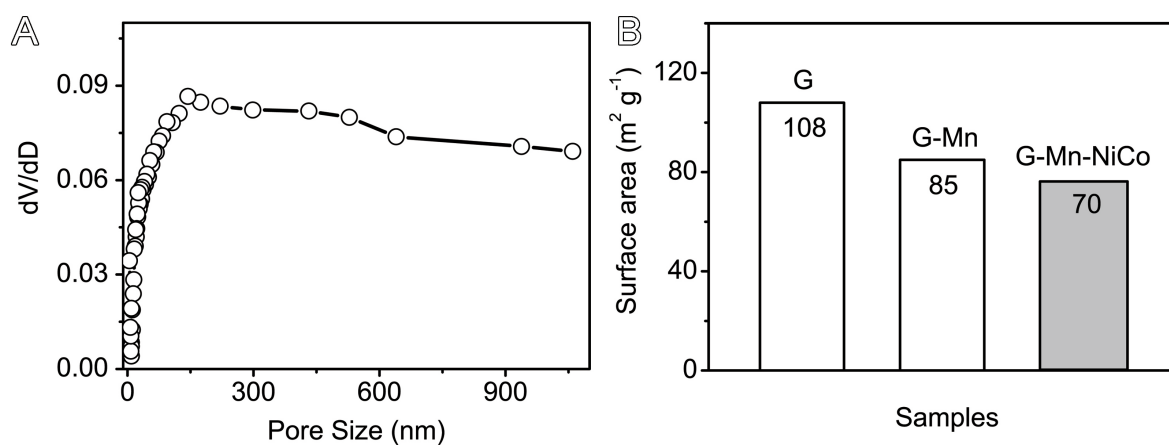


Figure S3. (A) pore size distribution (expressed in $cm^3 g^{-1} nm^{-1}$) of G-Mn-NiCo; (B) the surface area of samples calculated from MB experiments.

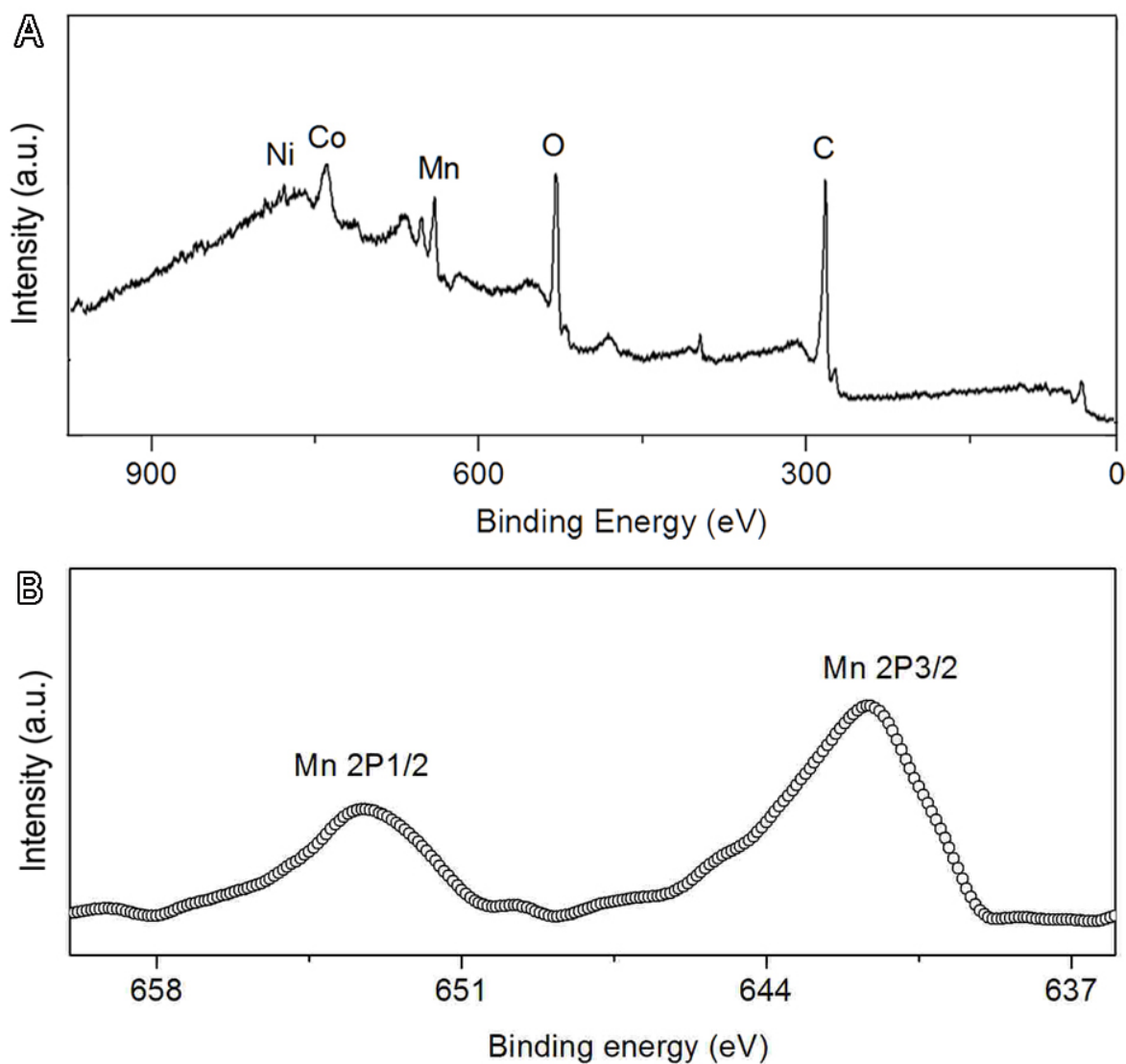


Figure S4. (A) XPS survey of G-Mn-NiCo; (B) Mn2p peaks of G-Mn XPS spectra.

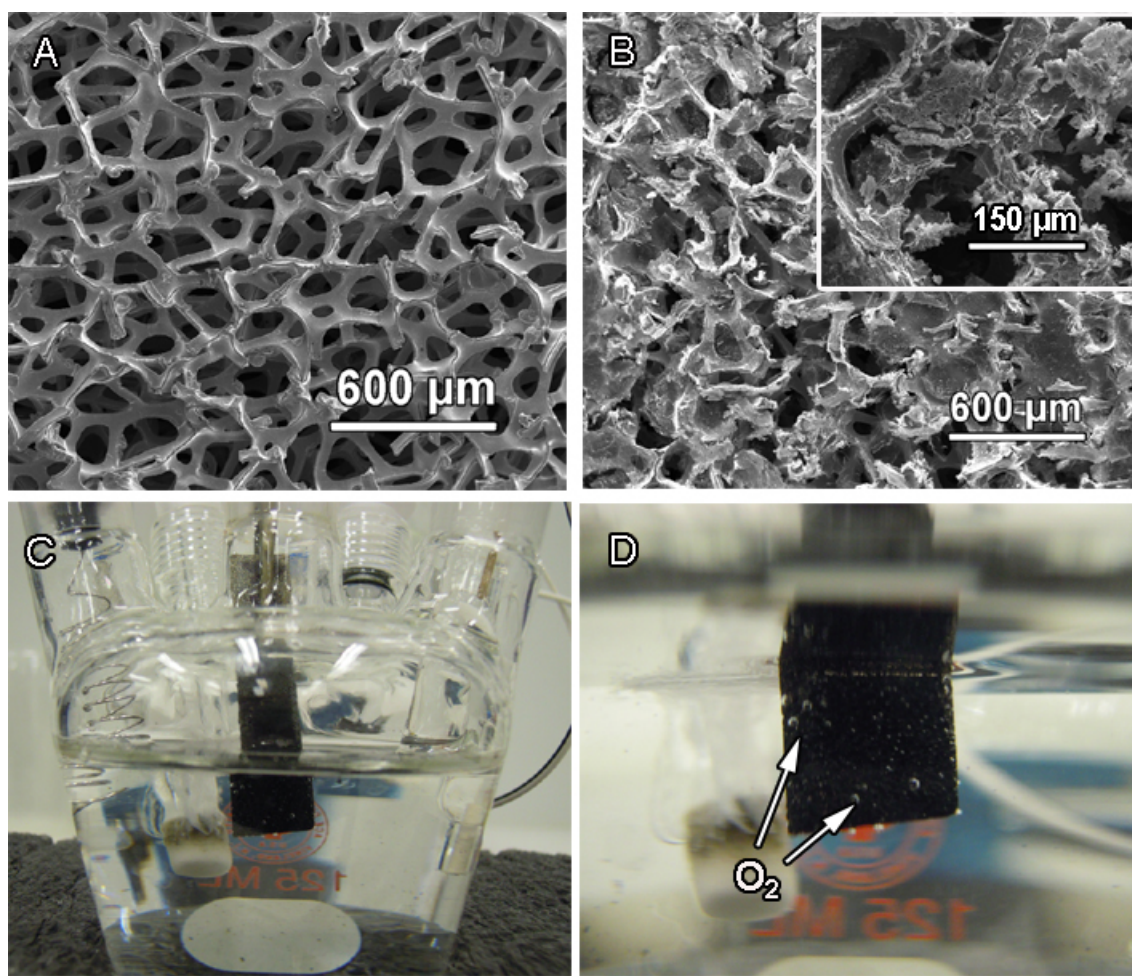


Figure S5. SEM images of nickel foam (A) and G-Mn-NiCo in nickel foam (B); (C) an optical image of the electrochemical cell; (D) an optical image of working electrode during operation at 0.7 V vs. Ag/AgCl; the bubbles indicate the formation of O₂ gas on working electrode.

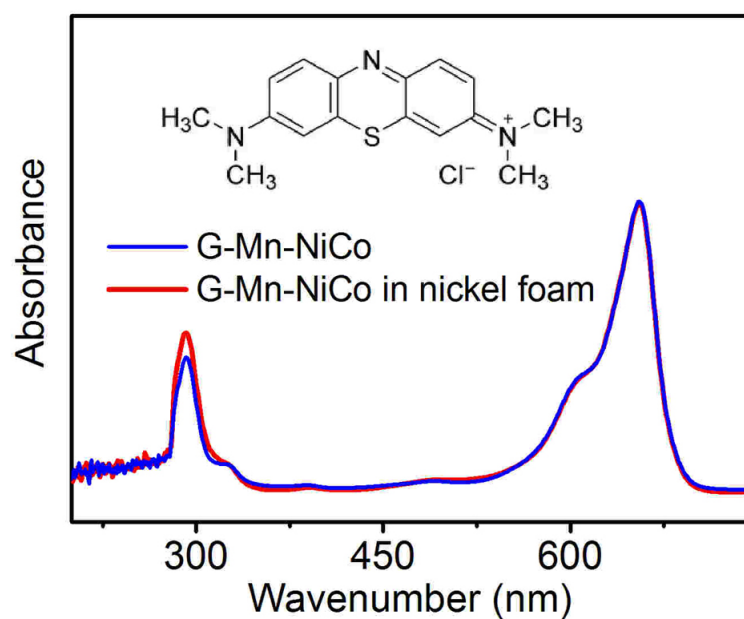


Figure S6 UV-vis spectra of G-Mn-NiCo and G-Mn-NiCo in nickel foam in MB experiments.

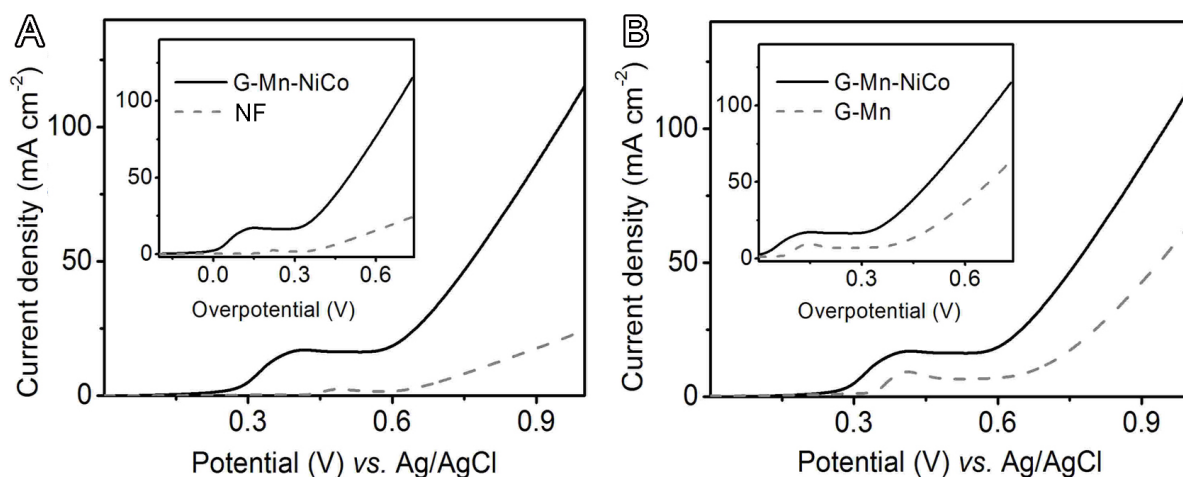


Figure S7. (A) LSV plots of G-Mn-NiCo and nickel foam (labeled as NF); (B) LSV plots of G-Mn-NiCo and G-Mn; the insets of (A) and (B) are the corresponding data re-plotted as the current density vs. overpotential.

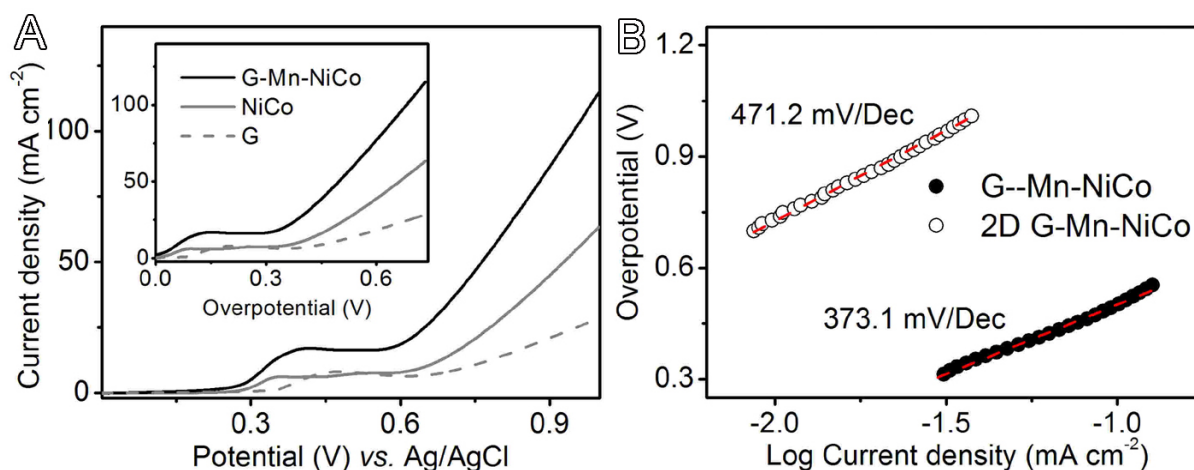


Figure S8. (A) LSV plots of G-Mn-NiCo, NiCo and G; the inset of (A) is the corresponding data re-plotted as the current density vs. overpotential; (B) Tafel plots of G-Mn-NiCo and 2D G-Mn-NiCo.

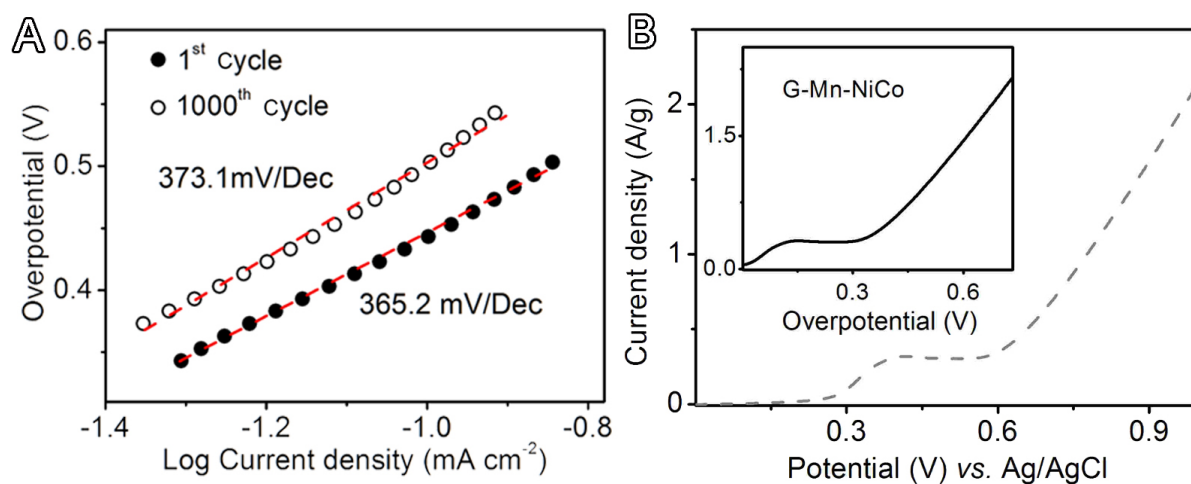


Figure S9. (A) Tafel plots of G-Mn-NiCo before and after 1000 cycles; (B) LSV plots of G-Mn-NiCo with the current density normalized with surface area; the inset is the corresponding data re-plotted as the current density vs. overpotential.

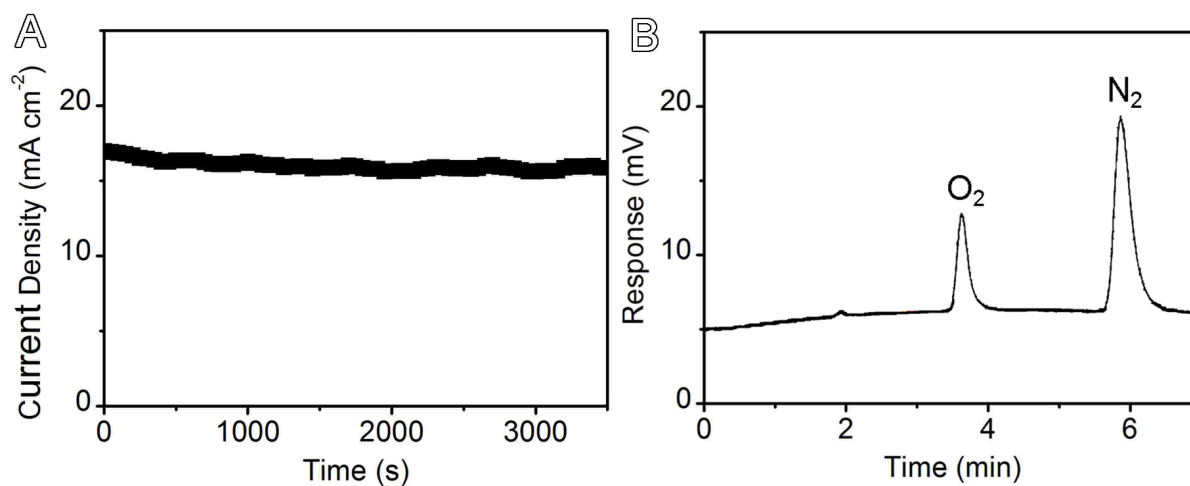


Figure S10 (A) Chronometric testing of G-Mn-NiCo for 60 min at 0.8 V vs. Ag/AgCl; (B) gas chromatography (GC) of as-produced oxygen.

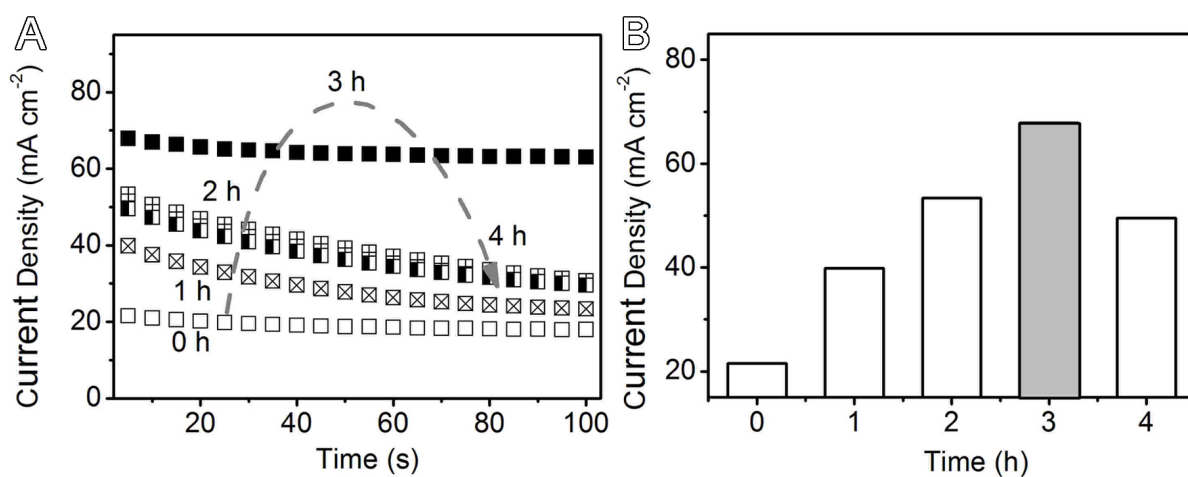


Figure S11. (A) Chronometric response for G-Mn-NiCo samples with different oxidation durations of KMnO_4 ; (B) the relationship of current density vs. oxidation duration of KMnO_4 .

References

- S1. W. S. Hummers and R. E. Offeman, *J. Am. Chem. Soc.*, 1958, **80**, 1339-1339.
- S2. P. T. Hang and G. Brindley, *Clays Clay Miner.*, 1970, **18**, 203-212.
- S3. M. F. El-Kady, V. Strong, S. Dubin and R. B. Kaner, *Science*, 2012, **335**, 1326-1330.
- S4. T. Tillotson and L. Hrubesh, *J. Non-Cryst. Solids*, 1992, **145**, 44-50.
- S5. M. Kruk, M. Jaroniec and A. Sayari, *Langmuir*, 1997, **13**, 6267-6273.
- S6. J. Chen, K. Sheng, P. Luo, C. Li and G. Shi, *Adv. Mater.*, 2012, **24**, 4569-4573.
- S7. B. Seger and P. V. Kamat, *J. Phys. Chem. C*, 2009, **113**, 7990-7995.
- S8. M. Grden, M. Alsabet and G. Jerkiewicz, *ACS. Appl. Mater. Interf.*, 2012, **4**, 3012-3021.